NANO LETTERS

Letter

pubs.acs.org/NanoLett

Single-Molecule Junctions with Epitaxial Graphene Nanoelectrodes

Konrad Ullmann,[†] Pedro B. Coto,[‡] Susanne Leitherer,[‡] Agustín Molina-Ontoria,[§,∥] Nazario Martín,[§] Michael Thoss,[‡] and Heiko B. Weber*[,†]

[†]Lehrstuhl für Angewandte Physik und Interdisziplinäres Zentrum für Molekulare Materialien, Friedrich-Alexander-Universität Erlangen-Nürnberg (FAU), Staudtstr. 7/A3, D-91058 Erlangen, Germany

[‡]Institut für Theoretische Physik und Interdisziplinäres Zentrum für Molekulare Materialien, Friedrich-Alexander-Universität Erlangen-Nürnberg (FAU), Staudtstr. 7/B2, D-91058 Erlangen, Germany

[§]Departamento de Química Orgánica, Facultad de Química, Universidad Complutense, E-28040 Madrid, Spain

[∥]IMDEA-Nanoscience, Campus de Cantoblanco, E-28049 Madrid, Spain

S *Supporting Information*

ABSTRACT: On the way to ultraflat single-molecule junctions with transparent electrodes, we present a fabrication scheme based on epitaxial graphene nanoelectrodes. As a suitable molecule, we identified a molecular wire with fullerene anchor groups. With these two components, stable electrical characteristics could be recorded. Electrical measurements show that single-molecule junctions with graphene and with gold electrodes display a striking agreement. This motivated a hypothesis that the differential conductance spectra are rather insensitive to the electrode material. It is further corroborated by the assignment of asymmetries and spectral features to internal molecular degrees of freedom. The demonstrated open-access graphene electrodes and the electrode-insensitive molecules provide a model system that will allow for a thorough investigation of an individual single-molecule contact with additional probes.

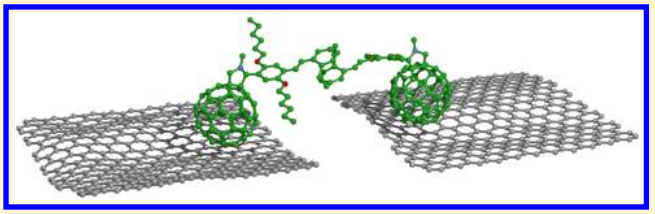

KEYWORDS: *Epitaxial graphene nanoelectrodes, electroburning, single-molecule junctions, fullerene end groups, switching*

How does charge flow across a single molecule? Since the first experiments in the late nineties,[1,2] scientists have been trying to answer this fundamental question. It is clear that the underlying physics is nontrivial and involves nonequilibrium electronic and vibronic phenomena.[3−8] Despite rapid experimental progress in the early years, the speed of innovation subsequently dropped considerably. The inherent experimental limitation is due to the metallic electrodes contacting the molecule. They provide two limits to the experiment:

The first is sample-to-sample variation of the electrical characteristics, which stems from the sensitivity to atomistic details, in particular in deformable gold contacts.[2] Because they seem unavoidable, many scientists have opted to study large ensemble measurements only, which allow for recognizing trends within the ensemble and compare them with trends in theoretical simulations. This approach has inherent limitations, as to understand charge flow through a single molecule, for which the thorough understanding of individual junctions remains all-important.

Another limiting feature of metallic electrodes is that they obscure the molecule from external access and impose significant constraints on the useful information derivable from experiments. External stimulation, for example with electrical fields or with electromagnetic radiation, will however be a key experiment to identify the underlying physical mechanisms of charge transport. For example, to study the influence of vibrations (which are known to have a strong impact in electron transfer as well as in optical spectroscopy of molecules), the resonant stimulation of specific modes with light would be a conclusive experiment that is prevented by the presence of the electrodes.

We pursue a redesign of the experiment, avoiding the problems inherent to metal electrodes. Instead of studying large ensembles of metal−molecule−metal contacts, we intend to study (again) individual contacts that are open for future parametric control due to light or other external stimuli. For this purpose, we replace the metal electrode pair by a thin epitaxial graphene electrode pair that is robust with respect to chemistry, intense light fields, and thermal cycling.

In this manuscript we present important steps in this direction: the reliable fabrication of graphene nanogaps and graphene−molecule−graphene junctions, which are ultraflat, transparent, robust, and in epitaxial registry.[9,10] As we will see, the results can immediately be linked to previous experiments.

The first step to use graphene nanoelectrodes for single-molecule junctions is the fabrication of numerous nanometer gapped electrode pairs. We use epitaxial graphene on 6H-SiC(0001), obtained by thermal decomposition of a SiC chip.[9]

Received: March 4, 2015
Revised: April 17, 2015

DOI: 10.1021/acs.nanolett.5b00877
Nano Lett. XXXX, XXX, XXX−XXX

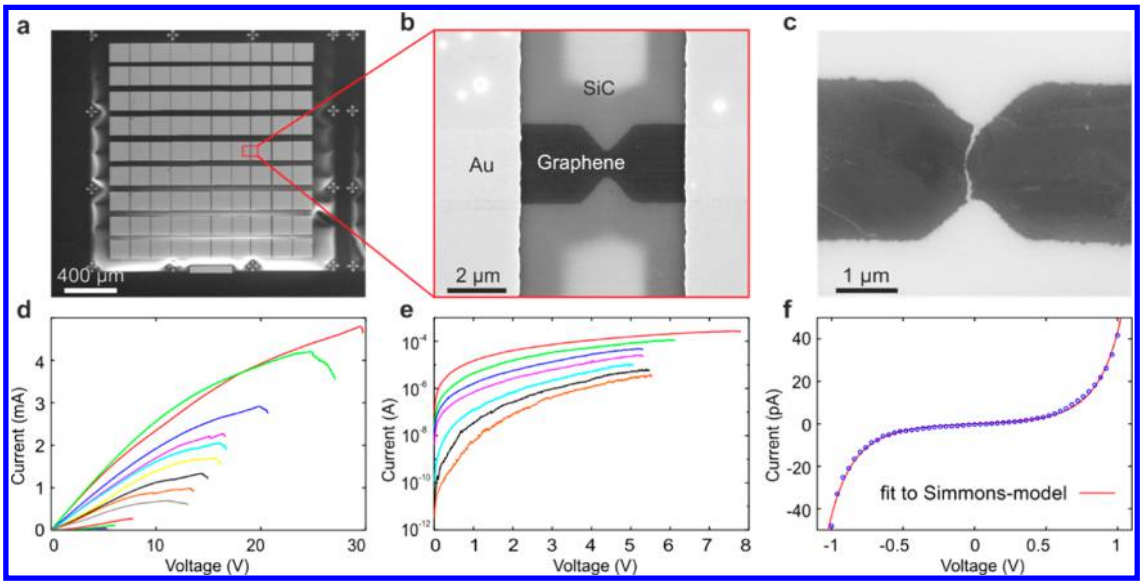

Figure 1. Formation of graphene nanojunctions: (a−c) SEM micrographs of the initial 81 epitaxial graphene microstrips (width at the narrowest point ∼1 μm, individually fitted with Au contact pads). Part c shows a typical device after formation of a nanogap. (d−e) The electrical breakdown protocol, carried out in ambient air, consists of a repeated sweep of the voltage, which is interrupted immediately as soon as the current drops and then restarted from zero voltage. This procedure is repeated up to a target resistance of ∼ GΩ. Part f displays the tunnel characteristics of such a junction (blue circles) and a computed tunnel characteristics.[13]

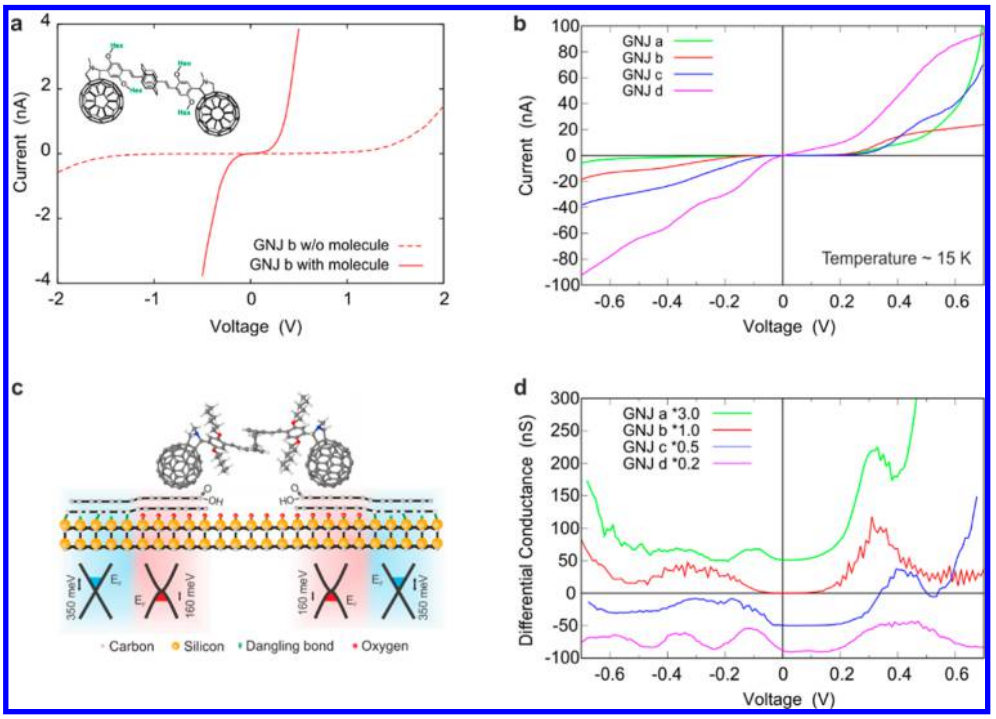

Figure 2. Single-molecule junctions with graphene nanoelectrodes: (a) C_{60} end-capped molecular wire, used for single-molecule junctions and tunnel characteristics of the same junction before (dashed) and after (solid line) application of molecules, recorded at room temperature. (b,d) Four graphene nanojunctions (GNJ) that display stable nonlinear electrical characteristics at low temperatures, which can be assigned to a single-molecule junction (see main text). The differential conductance in (d) is slightly rescaled and shifted by 50 nS each for better visibility. (c) Sketch of a GNJ bridged by a molecule. The graphene is presumably modified at its edge, both by end functionalization (typically with carboxylic groups) as well as by local intercalation with oxygen very close to the edge, which is induced during the formation of the nanojunction. As a consequence, the fullerene end group is expected to reside on a positively charged bilayer graphene area; see SI.

This high-quality material provides a finite electron density of $n = 10^{13}$ cm^{-2} and is in epitaxial registry with the monocrystalline wafer. An array of graphene microstrips (1 μm constriction width) is fabricated by standard e-beam lithography (Figure 1a−b), with metallic (Ti/Au) pads that give electrical access to individual microstrips. The nanogaps are fabricated by driving a substantial current through the microstrips in the presence of ambient air. A voltage V is ramped up to a level where the current suddenly drops. At this point, the voltage is rapidly switched off; the junction has now an increased resistance

DOI: 10.1021/acs.nanolett.5b00877
Nano Lett. XXXX, XXX, XXX−XXX

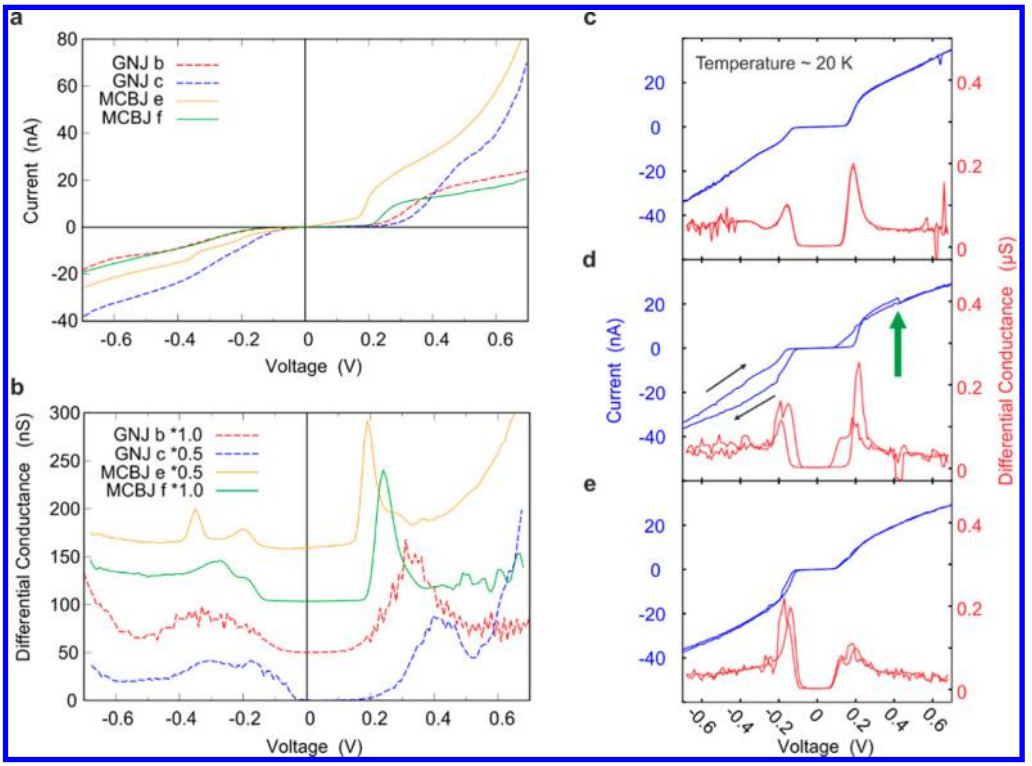

Figure 3. (a) Single-molecule junctions (raw data) using two different techniques: solid lines result from two independent measurements of single-molecule junction using gold electrodes (MCBJ). An asymmetric shape with a double peak at negative bias and a dominant peak at positive bias is found. The dashed curves are GNJ data. (b) Differential conductance derived thereof and rescaled/shifted for visibility. Most surprisingly, the IVs agree well for the two different electrode materials. The contact material appears to be exchangeable. (c–e) Three consecutive IV sweeps of an MCBJ displaying an inversion of the peak asymmetry. Due to the insensitivity of electrodes, this behavior can be attributed to an internal switching of the molecule in the junction.

(details are given in the SI). This procedure is repeated until resistances in the GΩ range are reached (cf. Figure 1d–e). Thus, narrow cracks are induced in the graphene microstrip, as shown by SEM imaging (Figure 1c). This protocol, for which the expression electroburning has been used, in contrast to electromigration, is similar to ref 11 (multilayer, exfoliated graphene) and ref 12 (nanotubes) but provides much narrower gaps, presumably because the excellent heat conduction in SiC allows for very local hot spots. Despite the ∼1 nm instrumental resolution of the SEM, the width of the gap at its narrowest part can hardly be characterized by SEM (the picture is in this area somewhat blurred and would suggest a gap of the order of 10 nm, which is an indicator of near-edge modification of epitaxial graphene, see SI). More meaningful for the characterization of the nanogaps' distance are tunneling IVs across the nanogap. Figure 1f shows typical IV characteristics: the current follows the well-known Simmons law,[13] that yields a distance of $d = 1.4 \pm 0.6$ nm for the given case ($\Phi = 0.6$ eV). The existence of a tunneling current and the shape of the IV strongly suggest that indeed a tunnel gap in the single nanometer range is achieved, even if the values determined by the Simmons formula should be taken cum grano salis. More importantly, this IV is not very sensitive to temperature variations. When cooling down the very same sample from room temperature to $T = 15$ K, $I(V)$ is reduced by a factor of 2–5 but remains stable in shape. Hence, we can exclude that current pathways through the semiconducting substrate are important. The residual T dependence is assigned to adsorbates or similar changes of the dielectric.

In a next step, molecules are applied to the chip from solution. We have opted for a fullerene end-capped molecule that comprises two styrene units that are covalently connected via a [2,2′]paracyclophane moiety in the center. Interestingly, the [2,2′]paracyclophane unit exhibits a remarkable π,π-interaction through the two parallel benzene rings, thus providing an efficient electronic communication, comparable to that observed for other π-conjugated oligomers.[14−16] Fullerene end-capped molecules have also been investigated in gold single-molecule junctions.[17−20]

The molecules are immersed in a 10^{-4} molar solution in CS_2. When the chip is removed from solution, it is blow-dried in a nitrogen stream. Subsequently, IVs are taken in vacuum at room temperature. It turns out that only a small fraction of the junctions experiences significant changes by the application of solvent and molecules. Among the 81 microstrips on one chip, 30–40 show a gap in the desired GΩ range. Among those, only few junctions show qualitatively different IVs with increased conduction like discussed below. The rest shows a slightly reduced tunneling-like electrical conduction and is not further investigated. This final yield is of the order of 5%. Among which only few have pronounced step-like features (see below). A blind experiment does not display qualitative changes upon immersion in pure solvent (see SI for detailed statistics).

In Figure 2a, the measured IVs of the very same junction is plotted before and after applying molecules, both at room temperature. Before application of molecules, this particular IV is slightly asymmetric but has nevertheless strong similarities to a tunneling IV. After application of molecules, the room temperature IV is strongly nonlinear with a threshold behavior at a few hundred meV (solid line in Figure 2a). The resulting IVs exhibit more detailed structures when the junction is cooled

DOI: 10.1021/acs.nanolett.5b00877
Nano Lett. XXXX, XXX, XXX−XXX

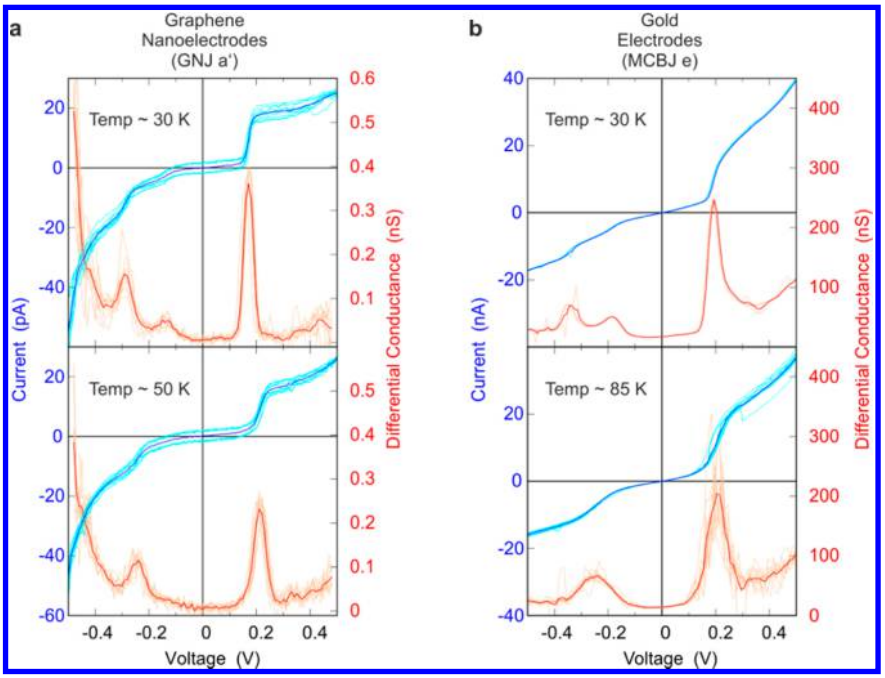

Figure 4. Temperature dependence of single-molecule junctions using two different electrodes: (a) GNJ, for which the strongly suppressed current level indicates a contact barrier and (b) MCBJ. The red and blue curves correspond to the average of single traces (pale red and pale blue) of the differential conductance and the current, respectively. Despite the very different electrodes, the low-T behavior (double peak at negative bias) and the elevated T behavior (merged peak) are common to both data sets. This further confirms that the spectra reflect properties of the molecular wire rather than the contact to the electrodes.

to T ~15 K (Figure 2b, red line) and have the overall shape of resonant tunneling with a blockade region at zero bias and broad peaks in the differential conductance (dI/dV), Figure 2d, together with further results under similar conditions. It is certainly surprising to see that all of those features are qualitatively similar to IVs recorded with low-temperature single-molecule junctions using gold electrodes and thiol-end-capped molecular wires.[6,21,22] We are convinced that these IVs are related to *single*-molecule contacts for the following reasons: (i) the strong similarity to IVs obtained with the mechanically controlled break junction (MCBJ) technique, (ii) nonlinear IVs are obtained with very low yield, when molecules in low concentration are applied; this finding makes larger numbers in the junction unlikely; (iii) Discrete switching behavior (cf. SI); (iv) asymmetries in the junction, which would average out when considering many-molecule contacts. Whether or not the molecule is free and isolated or in close contact with other molecules is currently unknown, but may, in principle, be imaged in future experiments, which is certainly a strength of the ultraflat graphene electrodes.

Figure 2b and d shows the $I(V)$ raw data, and the corresponding differential conductance dI/dV (rescaled by a correction factor 0.2−3 and shifted for better visibility) for all junctions with pronounced step-like features we measured so far. Common to all curves is a pronounced asymmetry, with a broader peak (sometimes double-peak) on one side (we defined this as negative bias), and a more pronounced peak on the opposite side. The curves display some sample-to-sample variations, but are all within a similar current range.

The similarity to previous findings encouraged us to try contacting the very same molecular species also in MCBJs.[2,21] Fullerene end groups are indeed well-suited to form stable contacts with gold nanotips.[23] Figure 3 a shows data obtained with the MCBJ technique and gold electrodes. The qualitative and semiquantitative agreement with the data on graphene nanojunctions becomes obvious when plotting both data in one single plot (Figure 3a and b): the solid lines correspond to the MCBJ (gold) data. The dashed lines correspond to selected graphene data. All features, including the overall current level, the lower, but broader peak (that sometimes appears as double peak) at negative bias, and the higher peak at positive bias are common. There are subtle differences between the curves. However, given the two different contact materials (with different work functions, see SI), the different bonding types and the different experimental techniques the agreement is stunning. This led us to the hypothesis that for such fullerene end-capped molecules, the electrode material is to a good approximation *exchangeable* (within the still existing sample-to sample variation).

This hypothesis is further corroborated by a measurement of a graphene based molecular junction GNJ a′. This junction was already presented as GNJ a, but was reinvestigated after 2 weeks in a different setup with improved temperature stability. The electrical characteristics appear strongly modified, in particular the current level has dropped by 3 orders of magnitude (Figure 4a). Noticeably, the IV characteristics display nevertheless very similar shape, compared to the other GNJs. The spectral similarity, together with the strong reduction of current, may indicate that the spectral features are defined by the molecule (which is considered to be intact), and the current level is reduced by an additional contact barrier, presumably between fullerene and graphene. With this junction, we performed temperature-dependent measurements. Figure 4a displays the junction at T = 30 K and at 50 K. The comparison yields a strong similarity of the overall shape, but the well distinguishable double peak at 30 K merges to a single, broadened peak at higher temperatures. When comparing the data with temperature-dependent results obtained with a

DOI: 10.1021/acs.nanolett.5b00877
Nano Lett. XXXX, XXX, XXX−XXX

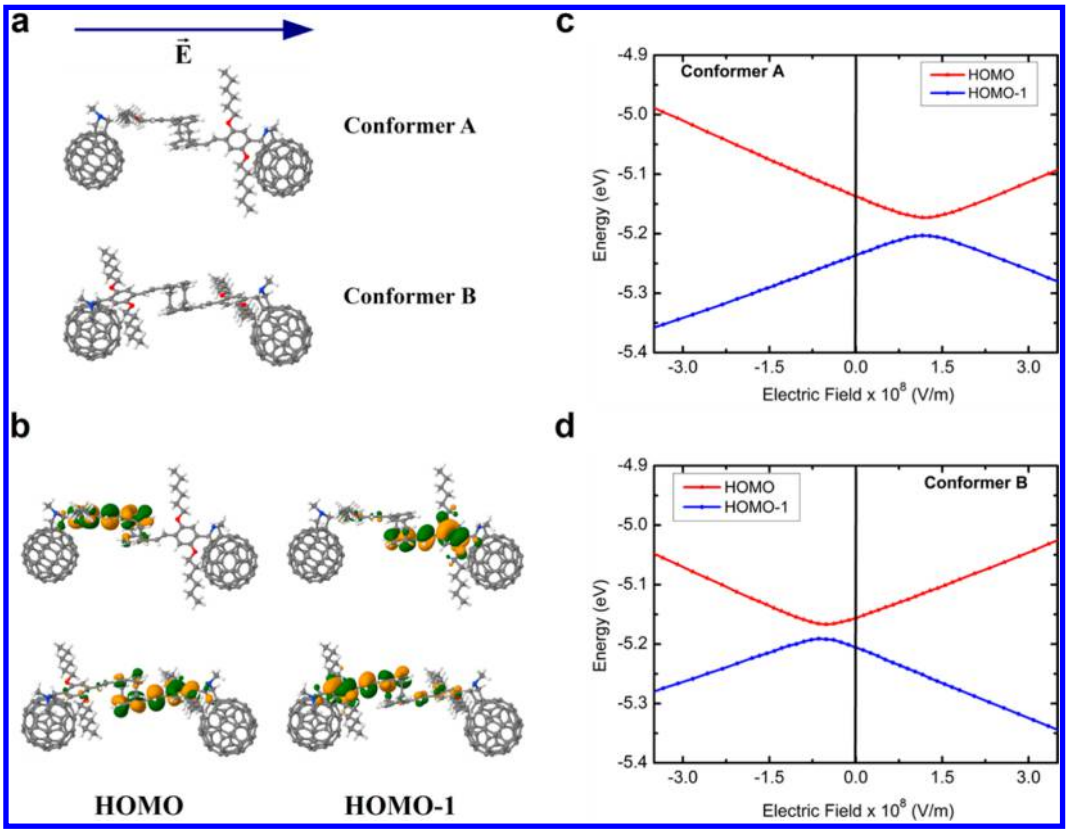

Figure 5. Conformers, orbitals, and their response to external fields: (a) Different conformations of the molecule investigated (conformers A and B) and direction of the external electric fields applied to simulate the bias potential in the junction. (b) HOMO and HOMO-1 of conformer A (top) and conformer B (bottom). Corresponding orbitals in both conformers localize in opposite sides of the molecule. (c,d) Energies of HOMO (red) and HOMO-1 (blue) as a function of the external electrostatic field applied for conformer A and B, respectively. The field dependence of the energy levels of the two conformers is similar for fields of equal strength applied in opposite directions. Therefore, a transition between the two conformations will revert the bias polarity dependence of the IV characteristic. For the conversion of the electric field to the corresponding bias voltage, see SI.

metal−molecule−metal junction (sample MCBJ e), the same qualitative behavior of a split peak at 30 K, but a single, broadened peak at higher temperature could be observed; see Figure 4b.

Altogether, despite the so far limited number of junctions investigated, IVs obtained with gold and graphene electrodes (the latter further with additional tunnel barriers) have so much in common that the above-mentioned hypothesis is well supported: *For the given molecule, the spectral features of the IVs are rather independent of the electrode material.* This is extremely astonishing, as formerly, very strong influence was ascribed to the specifics of the electrode material.[24]

In a next step, special attention is paid to the observed asymmetry in all IV characteristics. In metal−molecule−metal junctions, asymmetries were often assigned to contact asymmetries, which affect strongly the voltage drop, the charge transfer onto the molecule, etc.[2,25] For a critical test of the hypothesis, the appearance of asymmetries in the IV should be linked to an internal degree of freedom inside the molecule. Although the sequence of building blocks in the molecule is symmetric, the structure of the free molecule as determined by DFT calculations (cf. Figure 5) has no strict symmetry. The structural optimization reveals two geometric conformations (A and B, cf. Figure 5a) of the molecular bridge with similar energy, which differ in the relative orientation of the phenylenevinylene moieties in the central [2,2′]-paracyclophane-phenylenevinylene fragment. To assess the molecular origin of the asymmetry observed in IV characteristics, we have theoretically investigated the response of the electronic levels relevant for transport (HOMO and HOMO-1, see Figure 5b) to external electric fields applied in opposite directions. In this way, we model the effect of the electric field in the junction for different bias voltage polarity. As Figure 5c and d shows, the response of the levels to the external field depends profoundly on the bias polarity. In particular, the minimal energy difference between the two orbitals occurs for a finite electric field corresponding to a positive (negative) bias for conformer A (B). Since the two relevant levels correspond to π-orbitals localized at the two fragments of the molecular bridge, a small energy difference (quasi degeneracy) facilitates transport across the molecule. Indeed calculated transmission functions (not shown) indicate an enhanced transmission for positive (negative) bias for conformer A (B). Thus, the observed asymmetry in the IV is a result of the built-in asymmetry of the molecular bridge in combination with the existence of two π-systems separated by a barrier.

Strikingly, the field dependence of the energy levels of the two conformers interconvert upon change of the bias polarity. This indicates that a transition between the two conformations would revert the bias polarity dependence of the IV. Indeed, in the experiments we have observed the transition from a given asymmetry (higher peak at positive bias) to the opposite asymmetry (higher peak at negative bias) during three consecutive bias sweeps (Figure 3c−e). Indicated by a green

DOI: 10.1021/acs.nanolett.5b00877
Nano Lett. XXXX, XXX, XXX−XXX

arrow in Figure 3d, a sudden switch to an altered IV with reverse characteristics was detected in a gold MCBJ junction. This finding is certainly not due to a full rotation of the molecule (with an exchange of the fullerene ends) but must stem from a configuration change at fixed fullerene position, presumably from configuration A to configuration B, as suggested by the theoretical results. This finding gives further support to the hypothesis of weak sensitivity to contacts: asymmetries, and switching can be traced back to intrinsic properties of the molecule. This underscores the high quality of the experimental data.

In summary, we present the reliable formation of epitaxial graphene nanojunctions, which benefit from the excellent quality and availability of the graphene material and the exceptional heat conduction of the SiC substrate. These nanoelectrodes have further been used for the formation of single-molecule junctions with fullerene end-capped molecules. Those molecules are—within the limited data set presently available—surprisingly insensitive to the electrode material. In this spirit, the observed switching can be assigned to two conformers of the molecule, which are identified by ab initio calculations.

Our results suggest that the fullerene/graphene combination is excellently suited for substantially improved experiments on individual single-molecule junctions: graphene nanoelectrodes are ultraflat, transparent, and robust; they enable unprecedented access to the junction by additional techniques. We anticipate that manipulation and imaging with scanning probe tips, as well as detection and control with external fields,[26,27] is facilitated. In addition, chemical access from the gas phase or the liquid phase is now possible without steric hindrance by bulky gold electrodes. As a last example, temperature sweeps that do not affect the electrode distance[4] are now possible. Both fullerene end groups and epitaxial graphene electrodes will boost experimental progress in the field of single-molecule junctions.

Methods. The fabrication of the nanogaps and single-molecule junctions is described in the main text and in the SI. The ab initio optimizations were carried out using density functional theory (DFT) employing the Perdew–Burke–Emzerhof (PBE)[28] exchange-correlation functional and the def-SV(P) basis set.[29] This level of theory was selected to compare with results obtained for the full graphene–molecule–graphene system simulated at the DFT level using periodic boundary conditions and the PBE correlation-exchange functional. To get a better estimate of the energies of the electronic levels of the molecule we carried out single point calculations using the B3LYP correlation-exchange functional[30,31] at the optimized geometries.

■ ASSOCIATED CONTENT

Supporting Information

Additional technical details that will be valuable for experimental reproduction, as well as the statistics of the experimental results. Further, a discussion of the electrodes' work functions and of the molecule's asymmetry is presented. The Supporting Information is available free of charge on the ACS Publications website at DOI: 10.1021/acs.nanolett.5b00877.

■ AUTHOR INFORMATION

Corresponding Author

*E-mail: heiko.weber@fau.de.

Notes

The authors declare no competing financial interest.

■ ACKNOWLEDGMENTS

The work was carried out in the framework of the Sonderforschungsbereich 953 Synthetic Carbon Allotropes, supported by DFG. Generous allocation of computing time at the computing centres in Erlangen (RRZE), Munich (LRZ), and Jülich (JSC) is gratefully acknowledged.

■ REFERENCES

(1) Reed, M. A.; Zhou, C.; Muller, C. J.; Burgin, T. P.; Tour, J. M. *Science* **1997**, *278* (5336), 252–254.
(2) Reichert, J.; Ochs, R.; Beckmann, D.; Weber, H. B.; Mayor, M.; von Lohneysen, H. *Phys. Rev. Lett.* **2002**, *88*, (17) 176804.
(3) Ratner, M. *Nat. Nano* **2013**, *8* (6), 378–381.
(4) Ballmann, S.; Hartle, R.; Coto, P. B.; Elbing, M.; Mayor, M.; Bryce, M. R.; Thoss, M.; Weber, H. B. *Phys. Rev. Lett.* **2012**, *109* (5), 056801.
(5) Tao, N. J. *Nat. Nano* **2006**, *1* (3), 173–181.
(6) Secker, D.; Wagner, S.; Ballmann, S.; Hartle, R.; Thoss, M.; Weber, H. B. *Phys. Rev. Lett.* **2011**, *106* (13), 4.
(7) *Nat. Nanotechnol.* **2013**, *8* (6), 385–9.
(8) Ward, D. R.; Corley, D. A.; Tour, J. M.; Natelson, D. *Nat. Nano* **2011**, *6* (1), 33–38.
(9) Emtsev, K. V.; Bostwick, A.; Horn, K.; Jobst, J.; Kellogg, G. L.; Ley, L.; McChesney, J. L.; Ohta, T.; Reshanov, S. A.; Rohrl, J.; Rotenberg, E.; Schmid, A. K.; Waldmann, D.; Weber, H. B.; Seyller, T. *Nat. Mater.* **2009**, *8* (3), 203–207.
(10) Lauffer, P.; Emtsev, K. V.; Graupner, R.; Seyller, T.; Ley, L.; Reshanov, S. A.; Weber, H. B. *Phys. Rev. B* **2008**, *77* (15), 155426.
(11) Prins, F.; Barreiro, A.; Ruitenberg, J. W.; Seldenthuis, J. S.; Aliaga-Alcalde, N.; Vandersypen, L. M. K.; van der Zant, H. S. J. *Nano Lett.* **2011**, *11* (11), 4607–4611.
(12) Marquardt, C. W.; Grunder, S.; Blaszczyk, A.; Dehm, S.; Hennrich, F.; Lohneysen, H. v.; Mayor, M.; Krupke, R. *Nat. Nano* **2010**, *5* (12), 863–867.
(13) Simmons, J. G. *J. Appl. Phys.* **1963**, *34* (6), 1793–1803.
(14) Seferos, D. S.; Trammell, S. A.; Bazan, G. C.; Kushmerick, J. G. *Proc. Natl. Acad. Sci. U.S.A.* **2005**, *102* (25), 8821–8825.
(15) Molina-Ontoria, A.; Wielopolski, M.; Gebhardt, J.; Gouloumis, A.; Clark, T.; Guldi, D. M.; Martín, N. *J. Am. Chem. Soc.* **2011**, *133* (8), 2370–2373.
(16) Wielopolski, M.; Molina-Ontoria, A.; Schubert, C.; Margraf, J. T.; Krokos, E.; Kirschner, J.; Gouloumis, A.; Clark, T.; Guldi, D. M.; Martín, N. *J. Am. Chem. Soc.* **2013**, *135* (28), 10372–10381.
(17) Sørensen, J. K.; Fock, J.; Pedersen, A. H.; Petersen, A. B.; Jennum, K.; Bechgaard, K.; Kilså, K.; Geskin, V.; Cornil, J. R. M.; Bjørnholm, T.; Nielsen, M. B. *J. Org. Chem.* **2010**, *76* (1), 245–263.
(18) Markussen, T.; Settnes, M.; Thygesen, K. S. *J. Chem. Phys.* **2011**, *135* (14), -.
(19) Bilan, S.; Zotti, L. A.; Pauly, F.; Cuevas, J. C. *Phys. Rev. B* **2012**, *85* (20), 205403.
(20) Leary, E.; González, M. T.; van der Pol, C.; Bryce, M. R.; Filippone, S.; Martín, N.; Rubio-Bollinger, G.; Agraït, N. S. *Nano Lett.* **2011**, *11* (6), 2236–2241.
(21) Reichert, J.; Weber, H. B.; Mayor, M.; von Lohneysen, H. *Appl. Phys. Lett.* **2003**, *82* (23), 4137–4139.
(22) Ballmann, S.; Hieringer, W.; Secker, D.; Zheng, Q.; Gladysz, J. A.; Goerling, A.; Weber, H. B. *ChemPhysChem* **2010**, *11* (10), 2256–2260.
(23) Martin, C. A.; Ding, D.; Sørensen, J. K.; Bjørnholm, T.; van Ruitenbeek, J. M.; van der Zant, H. S. J. *J. Am. Chem. Soc.* **2008**, *130* (40), 13198–13199.
(24) Kim, T.; Vázquez, H.; Hybertsen, M. S.; Venkataraman, L. *Nano Lett.* **2013**, *13* (7), 3358–3364.

DOI: 10.1021/acs.nanolett.5b00877
Nano Lett. XXXX, XXX, XXX–XXX

(25) Elbing, M.; Ochs, R.; Koentopp, M.; Fischer, M.; von Hanisch, C.; Weigend, F.; Evers, F.; Weber, H. B.; Mayor, M. *Proc. Natl. Acad. Sci. U.S.A.* **2005**, *102* (25), 8815−8820.
(26) Martin, C. A.; Ruitenbeek, J. M. v.; Zant, H. S. J. v. d. *Nanotechnology* **2010**, *21* (26), 265201.
(27) Ballmann, S.; Weber, H. B. *New J. Phys.* **2012**, *14*, 23028−23028.
(28) Perdew, J. P.; Burke, K.; Ernzerhof, M. *Phys. Rev. Lett.* **1996**, *77* (18), 3865−3868.
(29) Schäfer, A.; Huber, C.; Ahlrichs, R. *J. Chem. Phys.* **1994**, *100* (8), 5829−5835.
(30) Vosko, S. H.; Wilk, L.; Nusair, M. *Can. J. Phys.* **1980**, *58* (8), 1200−1211.
(31) Lee, C.; Yang, W.; Parr, R. G. *Phys. Rev. B* **1988**, *37* (2), 785−789.

DOI: 10.1021/acs.nanolett.5b00877
Nano Lett. XXXX, XXX, XXX−XXX